American Mineralogist, Volume 93, pages 1424–1428, 2008

Equation of state and crystal structure of a new germanate post-titanite phase

FABRIZIO NESTOLA,[1,2,*] PÉTER NÉMETH,[3,4] ROSS J. ANGEL,[5] AND PETER R. BUSECK[4,6]

[1]Dipartimento di Geoscienze, Università di Padova, Via Giotto 1, I-35137, Padova, Italy
[2]CNR-IGG, Sezione di Padova, Via Giotto 1, I-35137, Padova, Italy
[3]Chemical Research Center of the Hungarian Academy of Sciences, Pusztaszeri út 59-67, H-1025, Budapest, Hungary
[4]School of Earth and Space Exploration, Arizona State University, Tempe, Arizona 85287-1404, U.S.A.
[5]Virginia Tech Crystallography Laboratory, Department of Geosciences, Virginia Polytechnic Institute and State University, Blacksburg, Virginia 24061, U.S.A.
[6]Department of Chemistry/Biochemistry, Arizona State University, Tempe, Arizona 85287-1604, U.S.A.

ABSTRACT

The compressibility and crystal structure of a recently discovered post-titanite phase of $CaGe_2O_5$ was investigated by single-crystal X-ray diffraction to 8.6 GPa at room temperature in a diamond-anvil cell. Unit-cell parameters decrease non-linearly with increasing pressure and do not show any discontinuity in the pressure range investigated. The unit-cell volume decreases by about 4.6% to 8.6 GPa. The *P-V* data were fit using a third-order Birch-Murnaghan equation of state giving the following coefficients: V_0 = 345.65(4) Å^3, K_{T0} = 159(1) GPa, and K' = 5.0(3). A parameterized form of the same equation of state was used to obtain the axial moduli for *a*, *b*, and *c*. The room-pressure ratios of axial compressibility are 2.64:1.00:1.42, indicating strong compression anisotropy, with *b* the stiffest direction and *a* the most compressible one. The crystal-structure data confirm that no change in symmetry occurs at high-pressure. Most of the compression to 8.6 GPa is accommodated by the CaO_8 and GeO_5 polyhedra, with reductions in volume of 5.6 and 4.6%, respectively. The analysis of the individual bond-lengths with pressure is discussed to explain the observed strong axial anisotropy. A comparison with the closely related crystal structure of andalusite shows that the post-titanite phase is less compressible by about 10%. A further comparison with other titanite phases studied at high-pressures allows us to obtain a qualitative model capable of predicting their bulk moduli when unit-cell volume at ambient conditions is known.

Keywords: Post-titanite, single crystal, high pressure, X-ray diffraction

INTRODUCTION

Many germanates show phase transformations similar to those of silicates but at lower pressures (e.g., Ross and Navrotsky 1988). Therefore, analogous germanates provide important information on the behavior of silicate minerals in the Earth's mantle, which may not be quenchable or readily studied within their *P-T* stability field. Recent discoveries include a new polymorph of $CaGe_2O_5$ with space group *Pbam*, which has a density at ambient conditions that is 5% greater than its low-pressure polymorph, which has a triclinically distorted titanite structure. The new phase, found to be stable above about 8 GPa and 1270 K, has been called post-titanite $CaGe_2O_5$ and its crystal structure was determined at ambient conditions (Németh et al. 2007). The discovery at high pressure of new phases, such as post-titanite $CaGe_2O_5$, clearly indicates that even if the chemistry of the mantle is well known, we cannot yet be confident that we have found all of the possible polymorphs that could occur under extreme conditions of temperature and pressure typical of Earth's mantle.

The aim of the current study was to determine the compressional and crystal-structure behavior of post-titanite $CaGe_2O_5$ using single-crystal X-ray diffraction. We discuss our results in comparison to andalusite, which is a closely related silicate structure, and to different titanite phases.

EXPERIMENTAL METHODS

A colorless single crystal of post-titanite $CaGe_2O_5$ from the study of Németh et al. (2007) was selected for high-pressure X-ray diffraction. An untwinned crystal measuring 150 × 75 × 45 μm was loaded in an ETH-type diamond cell (Miletich et al. 2000) using a T301 steel gasket, pre-indented to 90 μm with a hole of 250 μm diameter. A mixture of methanol:ethanol with a 4:1 ratio was used as a hydrostatic pressure-transmitting medium, and a crystal of quartz was loaded in the DAC together with the post-titanite sample as an internal pressure standard (Angel et al. 1997). Unit-cell parameters (Table 1) were determined at 10 different pressures up to about 8.6 GPa and room temperature on a Huber four-circle diffractometer (non-monochromatized Mo$K\alpha$ radiation) using eight-position centering of 16 Bragg reflections according to the procedure of King and Finger (1979). Centering procedures and vector-least-square refinement of unit-cell constants were performed using the SINGLE04 software (Angel et al. 2000) according to the protocols of Ralph and Finger (1982) and Angel et al. (1997). Unit-cell parameters measured in this work (Table 1) at room pressure are within 2–3 standard deviations of Németh et al. (2007); the differences are entirely attributable to differences in laboratory calibrations.

* E-mail: fabrizio.nestola@unipd.it

TABLE 1. Unit-cell parameters vs. pressure for post-titanite $CaGe_2O_5$ studied in this work

P (GPa)	a (Å)	b (Å)	c (Å)	V (Å³)
0.00010(1)*	7.306(2)	8.268(2)	5.714(1)	345.2(1)
0.00010(1)	7.3108(3)	8.2772(6)	5.7119(4)	345.64(2)
0.632(4)	7.2962(3)	8.2680(4)	5.7073(5)	344.30(3)
1.343(5)	7.2790(2)	8.2605(4)	5.7011(4)	342.80(2)
2.299(7)	7.2576(2)	8.2513(3)	5.6923(3)	340.88(2)
3.127(7)	7.2382(2)	8.2425(3)	5.6858(3)	339.22(2)
4.555(7)	7.2074(3)	8.2286(3)	5.6745(3)	336.53(2)
5.754(9)	7.1818(2)	8.2184(3)	5.6651(4)	334.37(2)
6.745(8)	7.1612(3)	8.2077(4)	5.6586(5)	332.59(3)
8.202(8)	7.1317(2)	8.1948(3)	5.6491(3)	330.15(2)
8.603(9)†	7.1236(2)	8.1912(3)	5.6469(3)	329.49(2)

* Data at ambient pressure from Nèmeth et al. (2007) reported for purpose of comparison.
† At this pressure, a complete intensity data collection was performed.

Intensity data were collected at 8.6 GPa and room temperature using a κ-geometry Xcalibur-2 diffractometer (Oxford Diffraction) with a point detector and graphite-monochromatized Mo$K\alpha$ radiation. The intensities were collected up to $2\theta_{max} = 80°$ using the ω-scan mode with a continuous-integrative step scan (0.05°/s, 60 scan steps, scan width 1.2°). The sample-detector distance was 135 mm. The intensity data were integrated using the program Win-IntegrStp (Angel 2003). The absorption correction for crystal, DAC, and gasket shadowing was performed using Absorb 6.0 (Angel 2004). Symmetry-equivalent reflection intensities were averaged and the outliers were rejected based on Average software (Angel 2006), resulting in 457 unique reflections. The crystal-structure refinement was performed using RFINE99, developed from a previous version, RFINE4 (Finger and Prince 1974), in space group *Pbam*. Atomic scattering factors and coefficients for dispersion correction were taken from the *International Tables for Crystallography* (Maslen et al. 1992; Creagh and McAuley 1992). The starting atomic coordinates were taken at ambient pressure from Németh et al. (2007). Crystal data, atomic coordinates, isotropic thermal parameter, selected bond lengths, and polyhedral volumes are reported in Tables 2, 3, and 4.

RESULTS

Equation of state

The variation of unit-cell parameters and volume as a function of pressure to 8.6 GPa is shown in Figure 1. The orthorhombic *a*, *b*, and *c* cell parameters decrease non-linearly with increasing pressure without discontinuities in the pressure range investigated. Unit-cell volume decreases by 4.6% to 8.6 GPa. No evidence for any phase transitions was observed to this pressure. The pressure-volume data were fit with a third-order Birch-Murnaghan equation of state (BM3-EoS) and the EOS-FIT5.2 software (Angel 2000) giving the following refined coefficients: $V_0 = 345.65(4)$ Å³, $K_{T0} = 159(1)$ GPa, and $K' = 5.0(3)$. The largest difference between the observed and calculated pressures is 0.022 GPa. The volume compressibility at room pressure, $\beta_V = -1/K_{T0}$, is thus -6.29×10^{-3} GPa^{-1}.

To determine the axial moduli for *a*, *b*, and *c* we used a parameterized form of the BM3-EoS using EoS-FIT5.2 in which the individual axes are cubed and fitted as volumes. All of the equation-of-state coefficients are reported in Table 5. The axial compressibilities, calculated using the relation for unit-cell parameters $\beta = -1/3K_{T0}$, gave values $\beta_a = -3.30 \times 10^{-3}$ (GPa^{-1}), $\beta_b = -1.25 \times 10^{-3}$ (GPa^{-1}), and $\beta_c = -1.77 \times 10^{-3}$ (GPa^{-1}), indicating that the post-titanite structure has strong elastic anisotropy at room pressure. The ratios of axial compressibilities are 2.64:1.00:1.42, with **b** being the stiffest direction.

Crystal-structure behavior at high pressure

The post-titanite phase is based on a network of two differently coordinated Ge polyhedra and 8-coordinated Ca sites.

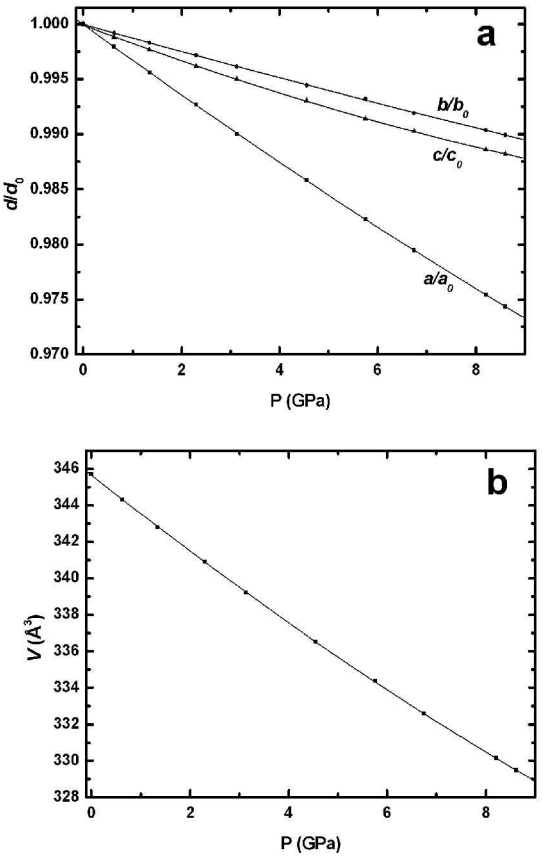

FIGURE 1. Relative compression d/d_0 for unit-cell parameters (**a**) and evolution of the volume with pressure (**b**) for post-titanite $CaGe_2O_5$. The errors are smaller than the symbols used.

TABLE 2. Summary of X-ray diffraction data for post-titanite $CaGe_2O_5$ measured at 8.609 GPa investigated in this work

Crystal data			
Space group	*Pbam*	*Z*	4
a (Å)	7.1236(2)	Formula weight M_r	265.26
b (Å)	8.1912(3)	Calculated density (g/cm³)	5.347
c (Å)	5.6468(3)	*F*(000)	496
V (Å³)	329.49(2)	Absorption coefficient μ (mm⁻¹)	19.682
Data collection			
Radiation type	Mo$K\alpha$	Measured refl.	457
Wavelength (Å)	0.71073	Observed refl.	341
$2\theta_{max}$	80°	Observed criterion	>2σ
Absorption correction	Absorb 6.0		
Monochromator	graphite	Measurement device	Xcalibur-2
Measurement method	ω scan		
Refinement			
Parameters refined	22	wR_{all}	0.037
R_{all}	0.065	wR_{obs}	0.033
R_{obs}	0.033	Goodness of fit (S)	1.15

One-half of the Ge atoms are 6-coordinated, forming the Ge1 octahedra, and the other half are 5-coordinated, forming the Ge2 square-based pyramids (Németh et al. 2007). The Ge1-octahedron occupies a site on the twofold axes parallel to [001] and thus has three independent Ge1-O bond distances. Its room-pressure volume is 9.04 Å³ at ambient conditions. At 8.6 GPa, the volume decreases to 8.78 Å³, a contraction of about 2.9%. The Ge2-pyramid lies on the mirror plane at $z = 0$, with

its apical O4 oxygen in the mirror plane. It thus includes three independent bond distances: Ge2-O1 (×2), Ge2-O2 (×2), and Ge2-O4. The O2-O2 edge of this pyramid is shared with an adjacent and symmetrically equivalent GeO_5 pyramid to form a Ge_2O_8 dimer (Fig. 2). This shared O2-O2 edge lies parallel to [001]. The polyhedral volume is 4.77 Å^3 at room pressure and decreases to 4.55 Å^3 at 8.6 GPa, a decrease of about 4.6%. The 8-coordinated Ca-polyhedron is characterized by three pairs of equivalent bond distances, Ca-O1$_{(short)}$, Ca-O1$_{(long)}$, and Ca-O2, in addition to two single Ca-O3$_{(short)}$ and Ca-O3$_{(long)}$ distances (see Table 4). The Ca-polyhedron is the most compressible since its volume decreases from 24.75 to 23.36 Å^3, or 5.6%. In terms of polyhedral linear compressibilities, the Ge1-octahedron shows $\beta = -3.34 \times 10^{-3}$ GPa^{-1}, the Ge2-pyramid has a $\beta = -5.36 \times 10^{-3}$ GPa^{-1}, and the Ca-polyhedron shows $\beta = -6.53 \times 10^{-3}$ GPa^{-1}. The analysis of the individual bond lengths indicate that most compressible ones are the Ca-O1$_{(long)}$ and Ca-O1$_{(short)}$, whereas the Ge1-O1 and Ge2-O1 are the stiffest (Table 4).

TABLE 3. Atomic coordinates and equivalent isotropic displacement parameters (U_{iso} in Å^2) for post-titanite $CaGe_2O_5$ relative to ambient conditions (Németh et al. 2007) and high pressure (this work)

P (GPa)	0.0*	8.6
Ge1		
x	0	0
y	0	0
z	0.25331(5)	0.2543(3)
U_{iso}	0.0045(2)	0.0044(5)
Ge2		
x	0.89175(4)	0.8918(2)
y	0.64576(4)	0.6468(1)
z	0	0
U_{iso}	0.0045(2)	0.0039(4)
Ca		
x	0.1355(1)	0.1313(3)
y	0.66590(9)	0.6663(3)
z	0.5	0.5
U_{iso}	0.0062(2)	0.0053(8)
O1		
x	0.1055(3)	0.1087(7)
y	0.2076(2)	0.2079(6)
z	0.2389(3)	0.243(2)
U_{iso}	0.0066(4)	0.005(2)
O2		
x	0	0
y	0.5	0.5
z	0.2071(5)	0.204(2)
U_{iso}	0.0074(5)	0.005(2)
O3		
x	0.1567(3)	0.161(1)
y	0.9446(3)	0.9439(9)
z	0.5	0.5
U_{iso}	0.0060(5)	0.005(3)
O4		
x	0.6564(3)	0.655(1)
y	0.5719(3)	0.575(1)
z	0	0
U_{iso}	0.0064(5)	0.005(2)

Note: The site occupancy factors are all 1.
* Data from Nèmeth et al. (2007).

TABLE 4. Selected interatomic distances (in Å) and polyhedral volumes for post-titanite $CaGe_2O_5$ relative to ambient conditions (Németh et al. 2007) and high pressure (this work)

P (GPa)	0.0	8.6	Variation (%)
Ge1-O1	1.884(2) ×2	1.872(5) ×2	−0.64
Ge1-O3	1.873(3) ×2	1.857(5) ×2	−0.86
Ge1-O4	1.938(2) ×2	1.916(5) ×2	−1.15
<Ge1-O>	1.898	1.882	−0.85
*V (Å^3)	9.04(2)	8.78(4)	−2.96
Ge2-O1	1.826(2) ×2	1.818(7) ×2	−0.44
Ge2-O2	1.868(2) ×2	1.834(8) ×2	−1.85
Ge2-O4	1.825(2)	1.784(7)	−2.30
<Ge2-O>	1.843	1.818	−1.38
*V (Å^3)	4.77(1)	4.55(3)	−4.84
Ca-O1$_{(short)}$	2.434(2) ×2	2.376(7) ×2	−2.44
Ca-O1$_{(long)}$	2.534(2) ×2	2.467(7) ×2	−2.72
Ca-O2	2.380(2) ×2	2.352(9) ×2	−1.19
Ca-O3$_{(long)}$	2.377(2)	2.347(8)	−1.28
Ca-O3$_{(short)}$	2.310(2)	2.283(8)	−1.18
<Ca-O>	2.424	2.378	−1.93
*V (Å^3)	24.75(4)	23.36(15)	−5.95

*As calculated in Balić-Žunić and Vickovic (1996).

DISCUSSION AND CONCLUDING REMARKS

Compressional behavior

The post-titanite $CaGe_2O_5$ has a crystal structure similar to that of andalusite, Al_2SiO_5. Both phases are orthorhombic: the post-titanite $CaGe_2O_5$ has *Pbam* and andalusite has *Pnnm* space-group symmetry (Fig. 2), and their unit-cell volumes are similar at ambient conditions [$V_{post\text{-}titanite}$ = 345.64(2) Å^3, this work, $V_{andalusite}$ = 341.93(2) Å^3, after Burt et al. 2006]. The different symmetries have no effect on the arrangement of the AlO_6 and GeO_6 octahedra (because they occupy special positions), and the positions of the edge-sharing octahedral chains parallel to [001] are the same (Fig. 2). These relationships lead to a remarkably similar structural arrangement when viewed in projection, if one considers the Ca in post-titanite $CaGe_2O_5$ to take the place of the Si in andalusite (Fig. 2). The differences between the two structures arise from the post-titanite having *b* and *a* glide planes parallel to (100) and (010), whereas andalusite has two *n* glide planes. As a consequence, in *Pbam* post-titanite all of the four 5-coordinated Ge atoms occupy positions at $z = 0$, whereas in *Pnnm* andalusite the *n* glides put two 5-coordinated Al at $z = 0$ and the other two at $z = 1/2$. Therefore, the structure of andalusite has a single type of mixed ^{V}Al and ^{IV}Si layer at both $z = 0$ and $z = 1/2$. By contrast, in post-titanite there are alternating layers of pure ^{V}Ge at $z = 0$ and pure Ca at $z = 1/2$. This similarity also means that the ^{V}Ge-^{V}Ge dimers in $CaGe_2O_5$ have a shared O2-O2 edge parallel to [001] to provide coordination to the Ca atoms in adjacent layers, whereas the adjacent ^{V}Al-^{V}Al dimers in andalusite have a shared edge that lies in the (001) plane so as to provide coordination to the Si atoms in the same layers. For a further comparison between the two structures we also report in Table 6 a list of the corresponding atomic coordinates.

This arrangement of layers, and the exchange of Ge for Al and

TABLE 5. Coefficients obtained by fitting a third-order Birch-Murnaghan EoS to the unit-cell parameters and volume of post-titanite $CaGe_2O_5$ studied in this work (see the text for details relative to the calculations)

a_0 (Å)	7.3111(3)	c_0 (Å)	5.7138(6)
$K_{T0,a}$ (GPa)	100.9(8)	$K_{T0,c}$ (GPa)	188(7)
K'_a	2.4(2)	K'_c	15(2)
β_a (×10^{-3} GPa^{-1})	−3.30	β_c (×10^{-3} GPa^{-1})	−1.77
b_0 (Å)	8.2744(3)	V_0 (Å^3)	345.65(4)
$K_{T0,b}$ (GPa)	267(2)	K_{T0} (GPa)	159(1)
K'_b	4(2)	K'	5.0(3)
β_b (×10^{-3} GPa^{-1})	−1.25	β_V (×10^{-3} GPa^{-1})	−6.29

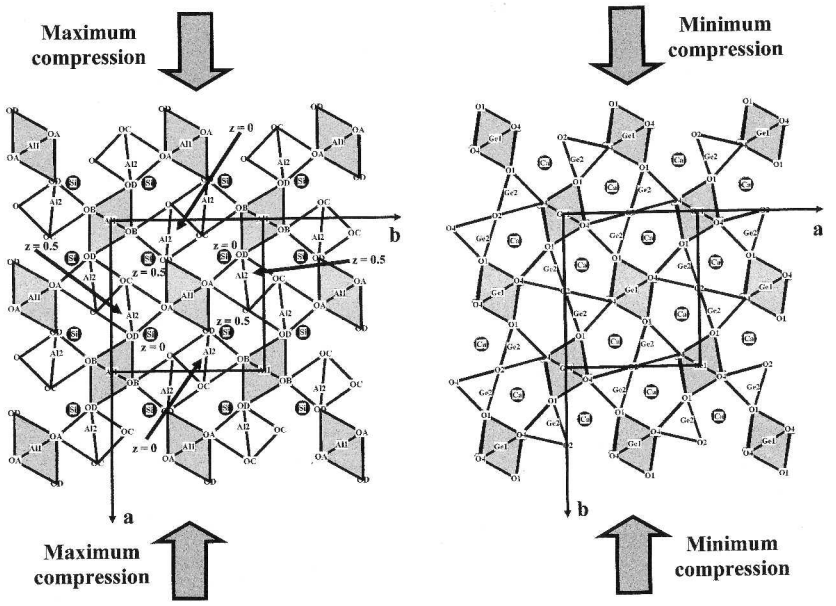

FIGURE 2. Polyhedral representations of the crystal structures of andalusite (left side, after Burt et al. 2006) and post-titanite $CaGe_2O_5$ (right side, after Nèmeth et al. 2007) at room pressure, both projected down the [001] direction. The *z*-coordinates of the Si and the Al2 atoms are indicated on the drawing of andalusite. In post-titanite $CaGe_2O_5$ all of the Ca atoms are at $z = 0.5$ and all of the Ge(V) are at $z = 0$.

Ca for Si, must be responsible for the large differences in elastic anisotropy between the two structures, even though their bulk moduli differ by no more than 10% [159(1) GPa for post-titanite $CaGe_2O_5$ against 144.2(7) GPa for andalusite (Burt et al. 2006)]. The *c* axis is about 20% softer in post-titanite $CaGe_2O_5$ than in andalusite, which can be attributed to two factors. First, the replacement of Al by Ge directly softens the octahedral chains. Second, in andalusite the consecutive AlO_6 octahedra are bridged along [001] by both the Al_2O_8 dimers and stiff SiO_4 tetrahedra that thereby support the octahedral chains. In contrast, the GeO_6 octahedral chains in post-titanite $CaGe_2O_5$ are bridged by Ge_2O_8 dimers and relatively soft Ca-O polyhedra. Put another way, the octahedral chains of andalusite are supported by stronger mixed Al,Si layers, whereas in post-titanite the support is removed by the presence of soft Ca-only layers, which negate any stiffening from the alternating layers of Ge_2O_8 dimers.

Within the (001) planes, the compressional anisotropy of the two phases is reversed, as the stiffer *b*-axis [152(1) GPa] of andalusite corresponds to the softer *a* axis [101(1) GPa] of post-titanite $CaGe_2O_5$, whereas the softer *a* axis [100(1) GPa] corresponds structurally to the stiffer *b* axis of post-titanite [267(2) GPa]. Previously, the compressional anisotropy of the (001) plane in andalusite has been explained as being a consequence of the soft All-OD bonds being aligned sub-parallel to [100], thus making the *a* axis substantially softer than the *b* axis. The corresponding Ge1-O1 bonds in post-titanite (which are aligned sub-parallel to [010]) are the stiffest in the structure, making the *b* axis stiffer than the *a* axis. Again, the layers of soft Ca-polyhedra in post-titanite $CaGe_2O_5$, because they are complete layers, are unable to support the remainder of the structure as the mixed layers of SiO_4 and AlO_5 polyhedra do in andalusite. In particular, the planes containing the two pairs Ca-$O1_{(short)}$ and Ca-$O1_{(long)}$ bonds are about 10° and 30°, respectively, from the **a** direction, which is the most compressible one in post-titanite $CaGe_2O_5$. A further contribution to the compression of *a* axis could also come from the Ge2-O4 distances, which show a strong contraction (Table 4). On the other hand the Ca-$O3_{(short)}$, Ge1-O1, and Ge2-O1 bond distances are those contributing to the high stiffness of the *b* axis, with a small contraction between 1.2 and 0.4%.

TABLE 6. Correspondence between the atomic coordinates for post-titanite $CaGe_2O_5$ and andalusite crystal structures at room pressure reported in Figure 3

	Post-titanite	Andalusite	Post-titanite	Andalusite
	Ca	Si	O2	OC
x	0.1355	0.2535	0	0.1017
y	0.6659	0.7524	0	0.4012
z	0.5	0.5	0.2071	0
	Ge1	Al1	O3	OA
x	0	0	0.1567	0.4224
y	0	0	0.9446	0.3638
z	0.2533	0.2418	0.5	0.5
	Ge2	Al2	O4	OB
x	0.8917	0.8703	0.6564	0.5746
y	0.6458	0.3612	0.5719	0.6381
z	0	0	0	0
	O1	OD		
x	0.1055	0.2292		
y	0.2076	0.1341		
z	0.2389	0.2388		

Bulk modulus vs. unit-cell volume: A qualitative model

Analysis of the literature data for different titanite phases investigated at high pressures leads to a linear relation between the bulk modulus, K_{T0}, and unit-cell volume at ambient conditions, V_0. Figure 3 shows data for $CaTiSiO_5$, $Ca(Ti_{0.5}Si_{0.5})SiO_5$, and $CaSi_2O_5$ from Angel et al. (1999), $CaGe_2O_5$ studied in this work, $CaSnSiO_5$ from Rath et al. (2003), and $CaTiSiO_5$ from Kunz et al. (2000). The linear relationship can be expressed as

$$K_{T0}\,(\text{GPa}) = 443(28) - 0.83(8) \times V\,(\text{Å}^3).$$

The correlation coefficient R for the linear trend is 0.98. Except for the germanate post titanite of this work, for which K' is close to 5, the value of K' for all the samples is close to 4.

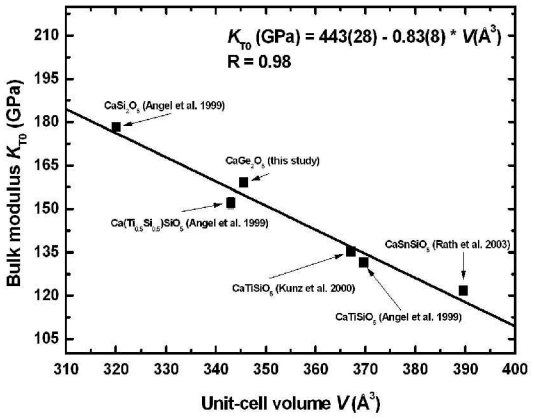

FIGURE 3. Unit-cell volumes V_0 vs. bulk modulus K_{T0} for titanite phases investigated at high pressure. The references are reported in the plot and in the text.

Therefore, for purpose of comparison, we calculated K_{T0} for post-titanite $CaGe_2O_5$ fixing K' to 4 and obtained a bulk modulus of 163 GPa, an increase by about 2.5% with respect to that refined with the BM3 in this work. The symbols shown in Figure 3 are large enough to contain such a difference in K_{T0}. It is apparent from this plot that the bulk modulus for post-titanite phases appears to fall on the same trend as that for titanite-structured materials, suggesting that to a first approximation the increase in bulk modulus expected for a titanite to post-titanite transition can simply be explained as a result of the increase in density.

AKNOWLEDGMENTS

The high-pressure diffraction experiments were performed at Virginia Tech Crystallography Laboratory, partially supported by NSF grant EAR-0408460. Financial support for Péter Németh at Arizona State University was provided by the Earth Sciences Division of the National Science Foundation via grant EAR-0440388. We thank S. Jacobsen and an anonymous referee for their helpful review and M. Kunz for his important suggestions.

REFERENCES CITED

Angel, R.J. (2000) Equation of state. In R.M. Hazen and R.T. Downs, Eds., High-temperature and High-pressure Crystal Chemistry, 41, 35–59. Reviews in Mineralogy and Geochemistry, Mineralogical Society of America, Chantilly, Virginia.

——— (2003) Automated profile analysis for single-crystal diffraction data. Journal of Applied Crystallography. Journal of Applied Crystallography, 36, 295–300.

——— (2004) Absorption corrections for diamond-anvil cells implemented in the software package Absorb 6.0. Journal of Applied Crystallography, 37, 486–492.

——— (2006) Average V2.2. A program to merge single-crystal diffraction intensity data, with rejection of outliers. Crystallography Laboratory, Department of Geological Sciences, Virginia Tech, Blacksburg, U.S.A.

Angel, R.J., Allan, D.R., Miletich, R., and Finger, L.W. (1997) The use of quartz as an internal pressure standard in high-pressure crystallography. Journal of Applied Crystallography, 30, 461–466.

Angel, R.J., Kunz, M., Miletich, R., Woodland, A.B., Koch, M., and Knoche, R.L. (1999) Effect of isovalent Si,Ti substitution on the bulk moduli of $Ca(Ti_{1-x}Si_x)SiO_5$ titanites. American Mineralogist, 84, 282–287.

Angel, R.J., Downs, R.T., and Finger, L.W. (2000) High-temperature, high-pressure diffractometry. In R.M. Hazen and R.T. Downs, Eds., High-temperature and High-pressure Crystal Chemistry, 41, p. 559–596. Reviews in Mineralogy and Geochemistry, Mineralogical Society of America, Chantilly, Virginia.

Balić-Žunić, T. and Vickovic, I. (1996) IVTON—program for the calculation of geometrical aspects of crystal structures and some chemical applications. Journal of Applied Crystallography, 29, 305–306.

Burt, J.B, Ross, N.L., Angel, R.J., and Koch, M. (2006) Equations of state and structures of andalusite to 9.8 GPa and sillimanite to 8.5 GPa. American Mineralogist, 91, 319–326.

Creagh, D.C. and McAuley, W.J. (1992) X-ray dispersion correction. In A.J.C. Wilson, Ed., International Tables for Crystallography, Vol. C, p. 206–219. Kluwer Academic Publishers, Dordrecht.

Finger, L.W. and Prince, E. (1974) A system of Fortran IV computer programs for crystal structure computations. U.S. National Bureau of Standards Technical Note 854.

King, H.E. and Finger, L.W. (1979) Diffracted beam crystal centering and its application to high-pressure crystallography. Journal of Applied Crystallography, 12, 374–378.

Kunz, M., Arlt, T., and Stolz, J. (2000) In situ powder diffraction study of titanite ($CaTiOSiO_4$) at high pressure and high temperature. American Mineralogist, 1465–1473.

Maslen, E.N., Fox, A.G., and O'Keefe, M.A. (1992) X-ray scattering. In A.J.C. Wilson, Ed., International Tables for Crystallography, Vol. C, p. 476–509. Kluwer Academic Publishers, Dordrecht.

Miletich, R., Allan, D.R., and Kuhs W.F. (2000) High-pressure single crystal techniques. In R.M. Hazen and R.T. Downs, Eds., High-temperature and High-pressure Crystal Chemistry, 41, p. 445–519. Reviews in Mineralogy and Geochemistry, Mineralogical Society of America, Chantilly, Virginia.

Németh, P., Leinenweber, K., Groy, T.L., and Buseck, P.R. (2007) A new high-pressure $CaGe_2O_5$ polymorph with five- and six-coordinated germanium. American Mineralogist, 92, 441–443.

Ralph, R.L. and Finger, L.W. (1982) A computer program for refinement of crystal orientation matrix and lattice constants from diffractometer data with lattice symmetry constraints. Journal of Applied Crystallography, 15, 537–539.

Rath, S., Kunz, M., and Miletich, R. (2003) Pressure-induced phase transition in malayaite, $CaSnOSiO_4$. American Mineralogist, 88, 293–300.

Ross, N.L. and Navrotsky, A. (1988) Study of the $MgGeO_3$ polymorphs (orthopyroxene, clinopyroxene, and ilmenite structures) by calorymetry, spectroscopy, and phase equilibria. American Mineralogist, 73, 1355–1365.

MANUSCRIPT RECEIVED AUGUST 28, 2007
MANUSCRIPT ACCEPTED JANUARY 24, 2008
MANUSCRIPT HANDLED BY MARTIN KUNZ